11th Australasian Fluid Mechanics Conference
University of Tasmania, Hobart, Australia
14-18 December 1992

SWIRLING FLOW IN A STRAIGHT DRAFT TUBE WITH ANNULAR AND RECTANGULAR CROSS SECTION

Toshiaki KANEMOTO[1], Takashi KUBOTA[2] and Haruo ISHIBASHI[1]

[1]Kyushu Institute of Technology, Tobata, Kitakyushu 804, JAPAN

[2]Kanagawa University, Kanagawa, Yokohama 221, JAPAN

ABSTRACT

The paper reports an experimental study concerning the effect of swirling flow on the internal flow structure and the performance of a straight diffuser for bulb turbines, whose cross section varies from annular to rectangular shape. In a transitional cross section, the swirl velocity is strong on the flat wall and weak at the concave corner. The through flow velocity is large at the concave corner. The swirl flow markedly increases the hydraulic loss in the inlet annular diffuser. On the contrary, the pressure recovery in the transitional diffuser increases with increasing swirl flow.

1. INTRODUCTION

To cope with the warming global environment, the development of the ultra-low head energy is active by welcoming as the clean and cool energy resources. Bulb turbines, which are suitable to the ultra-low head, have the very high velocity head at the inlet of draft tube, relative to the net head. Since the role of the draft tube on the hydraulic performance is extremely high, the bulb turbine normally uses a straight draft tube, which has an inlet annular diffuser followed by a diffuser having the transitional cross section from conical to rectangular shape.

The fact that the pertinent swirl flow suppresses the separation in the conical and annular diffusers has been reported by McDonald et al. (1971), Senoo et al. (1977), Kanemoto et al. (1981) and Tashiro et al. (1985). No paper, so far, is available concerning the effect of swirling flow on the flow structure in the draft tube for bulb turbines having the transitional cross section. The effect of swirl may differ from the results for axi-symmetric diffusers.

The authors present the experimental study by measuring the internal swirl flow through a model draft tube for bulb turbines to clarify the effect of swirl on the flow structure in the transitional cross sections, as well as the hydraulic performance.

2. MODEL DRAFT TUBE AND TEST PROCEDURE

<u>(2.1) Model Draft Tube</u>

Figure 1 shows the tested model draft tube with the inlet approach and downstream duct. Fig. 2 illustrates the cross sections viewing downstream on which the traverse lines for flow measurement are displayed. The twelve adjustable guide vanes [2] can generate the necessary swirl flow in place of the rotational runner. A stationary hub cone extends to the end of the annular diffuser [5]. The transitional diffuser [6] is followed by the rectangular downstream duct [7].

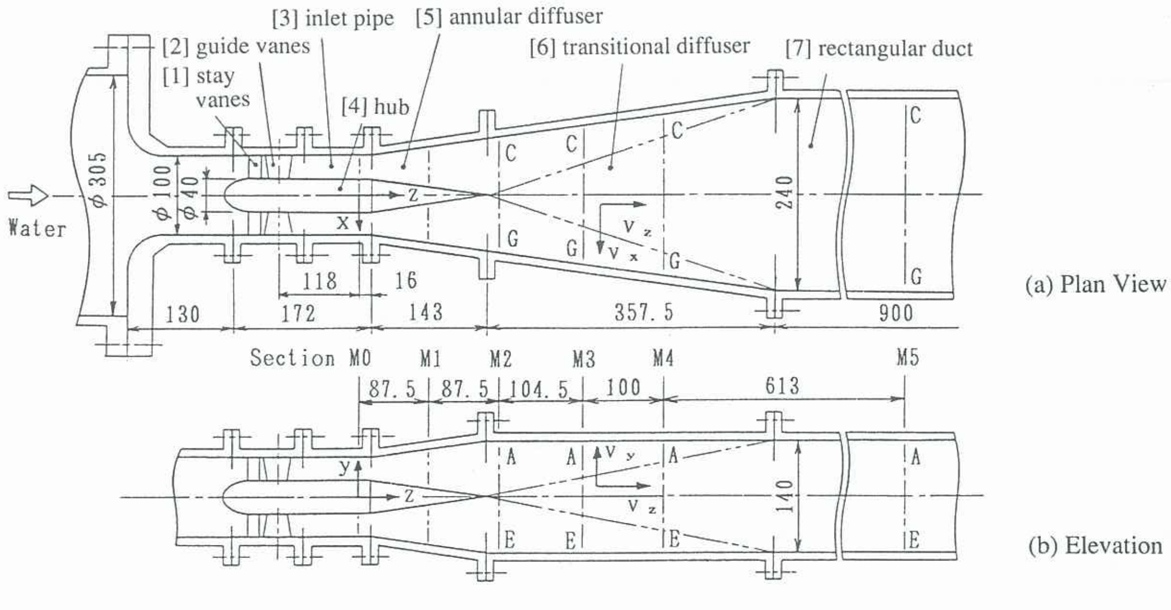

Fig. 1 Annular and Transitional Diffuser

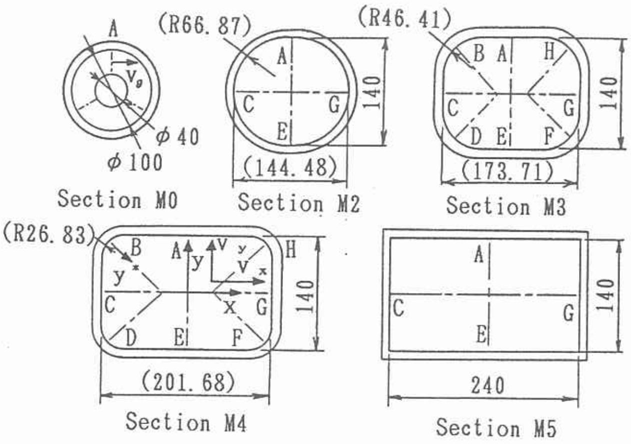

Fig. 2 Cross Sections Looking Downstream

(2.2) Test Procedure and Swirl Flow Conditions

The inflow swirl condition is determined from the flow profile measured at the reference cross section M0. The inflow swirl intensity m is obtained with the following equation:

$$m = \int r v_\theta v_z dA \Big/ \left(B_0 \int v_z^2 dA\right) \tag{1}$$

where v_θ and v_z are the swirl and axial velocity component at a radius r measured with a three-hole prove, and B_0 (=30 mm) the width of the passage. The axi-symmetry of measured flow profiles was good on the section M0. The test Reynolds number is 5.6 x 10^5 with the mean absolute velocity and the equivalent pipe diameter for the respective condition.

The four different intensities of swirling flow are selected: m of 0.03, 0.16, 0.22 and 0.48 that are hereafter described as F03 to F48. The typical flow profiles at the reference section M0 are shown in Fig. 3. The v_{z0} is the sectional averaged axial velocity. The negative value of v_θ denotes the counter-clockwise swirl looking downstream. The C_{Tz} is the total pressure coefficient:

$$C_{Tz} = \left(P_T - P_{T0}\right) \Big/ \left(\rho v_{z0}^2 / 2\right) \tag{2}$$

where P_T is the total pressure measured at the radius r, P_{T0} the mass averaged total pressure on the section M0, and ρ the density of water.

The discharges obtained by integrating the velocity profile in the sections M1 and M5 are within the 5 % of the discharge at M0. The discharge at the sections M2 to M4, where the flow fluctuates at the higher swirl intensity, are within the 15 %.

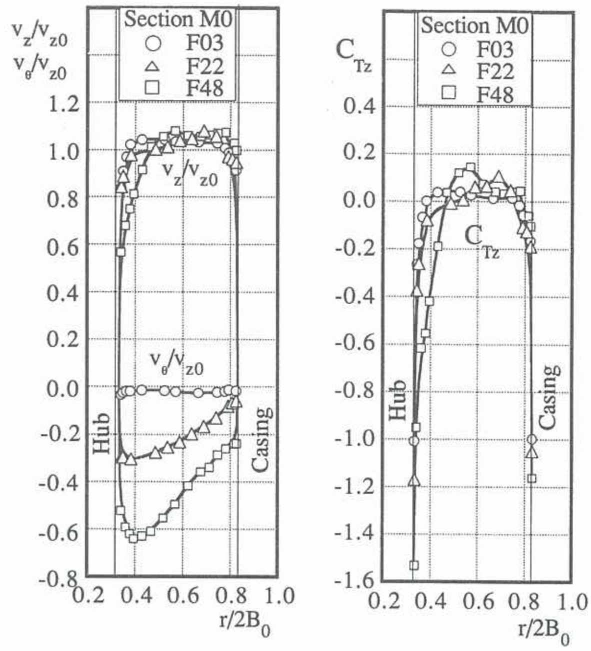

(a) Velocity Profiles (b) Total Pressure Profiles

Fig. 3 Flow Profile at Inlet Reference Section M0

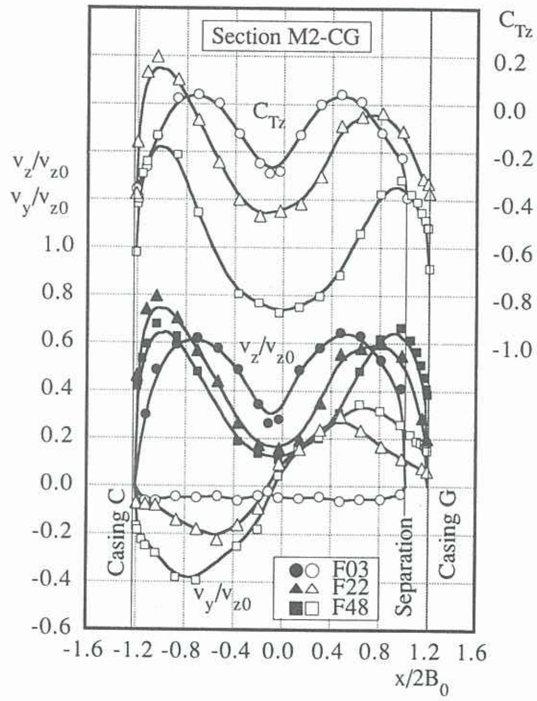

Fig. 4 Flow Profile at Section M2

3. FLOW PROFILES

(3.1) Swirl-Free Flow Profiles

Figures 4, 5 and 6 show the flow profiles in the sections M2, M4 and M5, respectively. The circular marks in the figures correspond to the almost swirl-free inflow F03 (m=0.03). The coordinates' systems for the traverse lines and velocity components refer to Fig. 2. The boundary layers develop on both walls in the section M2 at the inlet of transitional diffuser (Fig. 4). The flow separates from the right side wall G to the upper wall A. The main flow deviates towards bottom left. In a large central zone, the low energy flow exists due to the loss of velocity.

The central loss of velocity markedly recovers in the downstream section M4 (Fig. 5). The separated flow reattaches to the wall G, though the flow is still asymmetry. The clear negative swirl zone confines on the wall G. At the section M5 in the downstream rectangular duct (Fig. 6), the flow is uniform.

(3.2) Swirling Flow Profiles

In the section M2 (Fig. 4; triangular marks for F22 and squares for F48), the energy loss at the central zone becomes remarkable with increasing inlet swirl. The boundary layers on the outer walls become thinner in

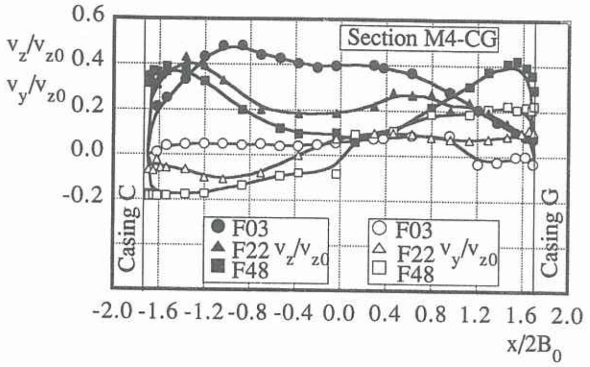

(a) Horizontal Distribution C-G

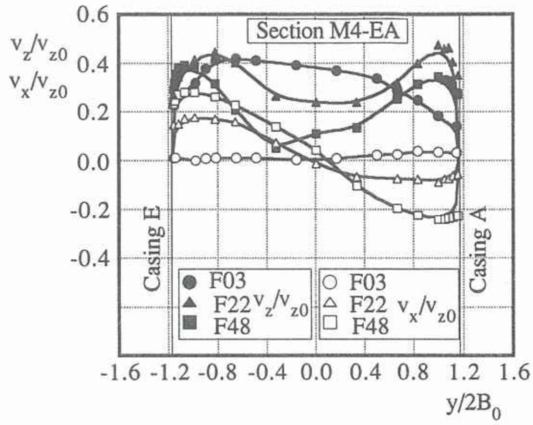

(b) Vertical Distribution E-A

Fig. 5 Velocity Profile at Section M4

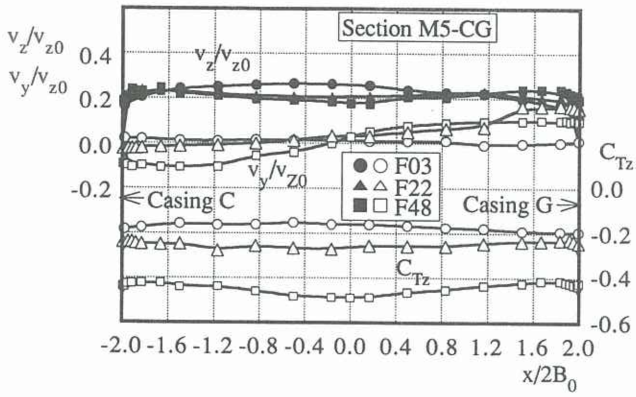

Fig. 6 Flow Profile at Section M5

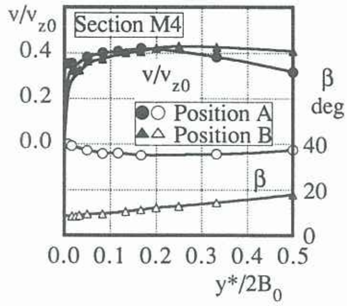

Fig. 7 Flow Profile at Wall and Corner (F48)

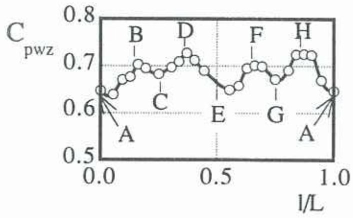

Fig. 8 Wall Pressure Distribution

this section, and the flow separation disappears with swirl. The flow profile in the section M4 becomes more symmetric with increasing swirl (Fig. 5). In the section M5 (Fig. 6), the reduction of the total pressure is noticeable with increasing swirl.

The swirl velocity profile is of free-vortex in the inlet section M0, and gradually transforms to the forced-vortex type in the downstream sections M2 to M5.

4. FLOW STRUCTURE IN TRANSITIONAL SECTION

Figure 7 compares the flow profiles at the mid position A of the upper flat wall (circular marks) and the position B at the upper left concave corner (triangular marks) in the section M4, when the swirl is the largest of F48. The v is the absolute velocity, β the flow angle measured from the axial direction (positive when the direction is the same as the main swirl), and y^* the perpendicular distance from the wall.

The flow angle at the corner is markedly smaller than the angle at the wall, keeping the same level of absolute velocity. This implies that the concave corner suppresses the swirl flow and increases the through flow in the transitional diffuser. The flow angle of A increases toward the wall, whereas the angle of B steadily decreases toward the corner. In other words, the swirl is stronger than the through flow on the flat wall and weaker at the concave corner.

In Fig. 5 (F48 of square marks), the maximum swirl velocities at the wider upper and lower walls of A and E are higher than those at the shorter side walls of C and G. On the other hand, the maximum axial velocities at the shorter walls are rather high compared with those at wider walls. Eventually, the maximum swirl velocity seems to be inversely proportional to the distance from the center of gravity to the respective position.

Figure 8 shows the wall pressures measured around the outer periphery of the cross section that is 60 mm upstream of the section M4. The wall pressure coefficient C_{Pwz} is

$$C_{P_{wz}} = \left(p_w - p_{w0}\right) / \left(\rho v_{z0}^2 / 2\right) \quad (3)$$

where p_w is the wall pressure (subscript $_0$ denotes the reference value in the section M0), l the distance along the outer periphery measured from point A, and L the total peripheral length. The swirl flow directs from A to H. The wall pressure is maximum at the respective corner B, D, F and H. The maximum pressures at the corners D and H, where the distance from the center of gravity transforms from longer to shorter, are higher than the pressures at the corners B and F where the distance changes from shorter to longer. On the contrary, the minimum pressure exists at the mid-point of the shorter walls C and G, as well as a little downstream of the mid-point of the wider walls A and E. The minimum pressures on the wider walls A and E

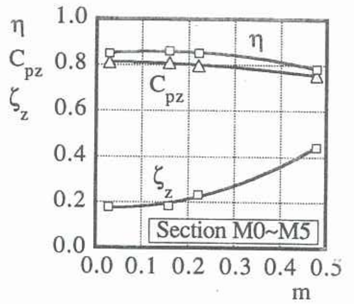

Fig. 9 Diffuser Performance

are lower than those on the shorter walls C and G. The pressure level at each position is inversely proportional to the swirl velocity.

Table I compare the displacement thickness δ^* and the shape factor H_s of the boundary layer along the wall of the section M4 at the swirl intensity F03 and F48. Different from the almost swirl-free flow F03, the boundary layer under the strong swirl F48 becomes markedly thinner around the whole periphery. Though the boundary layers at the corners are somewhat thicker than those at the walls, there is no clear difference in the shape factors.

Table I Boundary Layer on Wall in Section M4

Swirl	F03		F48	
Position	δ^* mm	Hs	δ^* mm	Hs
A	11.7	1.68	0.73	1.23
B	18.8	2.34	1.34	1.34
C	12.9	1.89	0.53	1.21
D	12.6	1.92	1.38	1.29
E	4.9	1.51	0.50	1.37
F	23.4	2.33	2.01	1.36
G	27.1	2.41	0.70	1.23
H	25.8	2.12	2.26	1.35

5. HYDRAULIC LOSS AND PRESSURE RECOVERY

(5.1) Loss and Performance of Whole Diffuser

The hydraulic loss coefficient ζ_z, the pressure recovery factor C_{pz} and the diffuser efficiency η between the inlet reference section M0 and the outlet section M5 can be obtained with the following equations:

$$\zeta_z = \left(P_{T_0} - P_{T_5}\right) / \left(\rho v_{z0}^2 / 2\right) \quad (4)$$

$$C_{pz} = \left(p_{m_5} - p_{m_0}\right) / \left(\rho v_{z0}^2 / 2\right) \quad (5)$$

$$\eta = \left(p_{m_5} - p_{m_0}\right) / \left[\rho \left(v_{z0}^2 - v_{z5}^2\right) / 2\right] \quad (6)$$

where P_T and p_m are the mass averaged total and static pressure. Figure 9 shows ζ_z (circular marks), C_{pz} (triangular marks) and η (square marks) versus the swirl intensity m. The hydraulic loss reaches minimum at around m of 0.1, and increases markedly at the high swirl intensity. The pressure recovery factor and efficiency also reach maximums at around m of 0.1, however, don't deteriorate so much at the higher swirl.

(5.2) Component Loss and Performance

The hydraulic loss, pressure recovery and efficiency of a whole diffuser are divided into those of an annular diffuser (from M0 to M2) and a transitional diffuser (from M2 to M5) for the inlet swirl conditions F03 and F48 as shown in Table II. The annular and transitional diffusers share the same level of hydraulic loss at almost swirl-free inflow. Under the high swirl, the increase of loss in the annular diffuser is remarkable. In the transitional diffuser, the loss reduces with swirl. Under the swirl-free inflow, the pressure recovery factor and efficiency of the annular diffuser is high. The contribution of the transitional diffuser and the downstream duct to the pressure recovery and efficiency is small at the swirl-free inflow, but is important when the swirl is increased.

Table II Breakdown of Performances

Swirl	F03		F48	
Section	M0 to M2	M2 to M5	M0 to M2	M2 to M5
ζ_z	0.084	0.094	0.356	0.087
C_{pz}	0.667	0.145	0.498	0.256
η	0.766	0.077	0.571	0.213

6. CONCLUSION

As a result of the experimental study of swirling flow through a straight draft tube having the transitional cross section from annular to rectangular shape, followings are clarified:

(1). In the rectangular cross section of the transitional diffuser, the maximum swirl velocity along the outer periphery is high on the wall, and low at the corner.

(2). The wall pressure varies along the periphery of the rectangular section inversely proportional to the maximum swirl velocity.

(3). At the concave corner of the rectangular section, the swirl velocity decreases and the through flow velocity increases.

(4). The hydraulic loss in the inlet annular diffuser markedly increases with increasing swirl. The loss in the transitional diffuser is rather reduced with swirl.

(5). The pressure recovery factor and the efficiency of the inlet annular diffuser reduce with increasing swirl. On the contrary, the pressure recovery factor and the efficiency of the downstream transitional diffuser become higher with increasing swirl.

REFERENCES

KANEMOTO, T, TOYOKURA, T and KUROKAWA, J (1982) Flow in Annular Diffusers. Bull. Japan Soc Mech Eng, 25-204, 912-918.

MCDONALD, A.T, FOX, R.W and VAN DEWOESTINE, R.V (1971) Effect of Swirling Inlet Flow on Pressure Recovery in Conical Diffusers. J of AIAA, 9-10, 2014-2018.

SENOO, Y, TAKEI, Y and NAGATA, T (1977) Swirling Flow in Conical Diffusers. Trans Japan Soc Mech Eng, 43-369, 1803-1810 (in Japanese).

TASHIRO, S and YOSHIKI, H (1985) Pressure Recovery Performance of Conical Diffusers in Swirling Flow. Trans Japan Soc Mech Eng, 51-462B, 486-493 (in Japanese).